Agora of Additive Manufacturing (2024) paper24006

Agora of Additive Manufacturing

journal homepage: http://additive-manufacturing.or.jp/

New nozzle cap to improve interlaminar strength of 3D-printed continuous carbon fiber composites

Akira Todoroki [a], Kota Hayakawa [a], Keisuke Iizuka [b]

[a] School of Engineering, Department of Mechanical Engineering, Tokyo Institute of Technology, Tokyo, Japan

[b] Faculty of Science and Technology, Department of Mechanical Engineering, Aoyama Gakuin University, Kanagawa, Japan

ABSTRACT

A new 3D printer hardware with coaxially arranged twin nozzles was developed to print continuous and short-fiber filaments. The short-fiber nozzle used a screw and pellets instead of filaments, and a hole was drilled at the center of the screw to print continuous fibers. The new coaxial 3D printer showed a 7% void area and low strength in the lay-up direction. Thus, in this study, a novel nozzle cap was designed to improve the performance of the aforementioned 3D printer. The nozzle cap transferred heat from the heat block to the printed path by extending the rim area of the nozzle edge. Printing tests were performed, and the void ratio was reduced to 2%. Interlaminar shear test results indicated that the interlaminar strength improved by 2.3 times.

Keywords: Carbon fiber, 3D printing, Twin nozzle system, Thermoplastic, Nozzle, Interlaminar strength

1. Introduction

At the Solid Works World Design Conference held in the U.S. in 2014, Markforged unveiled a 3D printer that molds thermoplastic composites reinforced with continuous carbon fibers using fused filament fabrication (FFF) [(1)]. Matsuzaki et al. [(2)] and Tian et al. [(3)] achieved a composite material molding device that impregnates carbon fibers with thermoplastic resin in the nozzle of FFF 3D printers.

Van Der Klift et al. [(4)] evaluated the tensile strength of continuous fiber composite–molded products using a Markforged 3D printer and reported that the void rate was approximately 7%. The tensile strength of various orientation specimens of continuous carbon fiber composites molded using Markforged 3D printer was reported by Todoroki et al. [(5)] Yamanaka et al. [(6)] proposed a method to reduce the stress concentration around the hole by placing the curved fiber bundles molded using a 3D printer.

However, using the Markforged 3D printer, the positions of the short-fiber or resin nozzle and the continuous-fiber nozzle are different, resulting in a large gap between adjacent print paths when the two adjacent print paths have different curvatures. Todoroki et al. [(7)] developed a new coaxial twin-nozzle 3D printer, and the new 3D printer enabled us to address the large gaps. The first nozzle prints short-fiber composites or thermoplastic resin using the screw-and-pellet method. The second nozzle is located in the center hole of the screw, and it prints the continuous fiber composites. However, the printed composites still have gaps between the printed paths, and the void ratio was as high as 7%, which was similar to that of Markforged 3D printers.

Ueda et al. [(8)] reduced the void rate by pressurizing with a heated metal roller, which was used immediately after printing the continuous composite paths. Imaeda et al. [(9)] improved the moving particle semi-implicit (MPS) method, which is a

* Corresponding author
Email: todoroki.a.aa@m.titech.ac.jp
Received 19 September 2024; Revised 30 October 2024; Accepted 1 November 2024
Available online 17 November 2024

type of particle method, and developed a method for analyzing the flow of thermoplastic resin in an FFF 3D printer that considers the heat of fusion as a composite material composed of fibers and thermoplastic resin. Kubota et al. [(10)] reported that by attaching a wide flat plate to the print head, the printed paths are heated by radiant heat, and the interlaminar strength is improved. The research has shown that the heating of printed paths caused fusion and bonding between the interlamina.

Therefore, in this study, a metal part (called a nozzle cap) that serves as an extension of the heating part around the nozzle was attached to the printer as the print head of the screw-type 3D printer is large. This nozzle cap can achieve sufficient melting and fusion of the printed pass, thereby reducing the voids between the print passes and improving the interlaminar strength. In this study, the effectiveness of the nozzle cap is experimentally verified by tensile tests and interlaminar shear tests.

2. Nozzle Cap

2.1 Basic concept of the screw coaxial double-nozzle printer

The outline of the print head of the screw-type coaxial twin-nozzle 3D printer proposed in the previous report [(7)] is shown in Fig. 1. The nozzle of the short-fiber-reinforced thermoplastic resin (or thermoplastic resin) and the nozzle of the continuous-fiber composites were arranged coaxially. The short fiber or thermoplastic resin was supplied as pellets, and the pellets were supplied using a screw. In addition, a thin hole was made at the center of the screw shaft, and a pipe was inserted into the hole. This pipe was arranged on the same axis as the continuous fiber nozzle and the screw. Figure 2 shows the configuration of the coaxial twin nozzles.

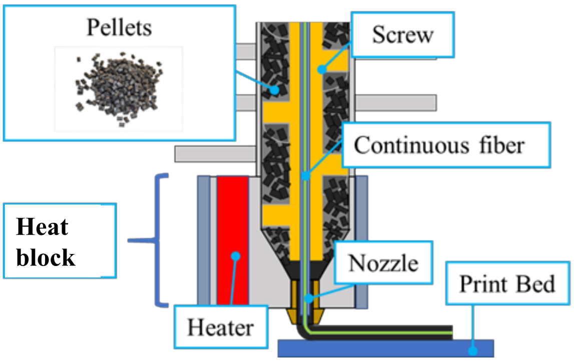

Fig. 1 Schematic representation of the new 3D printer. (Fig. 1 from reference [7])

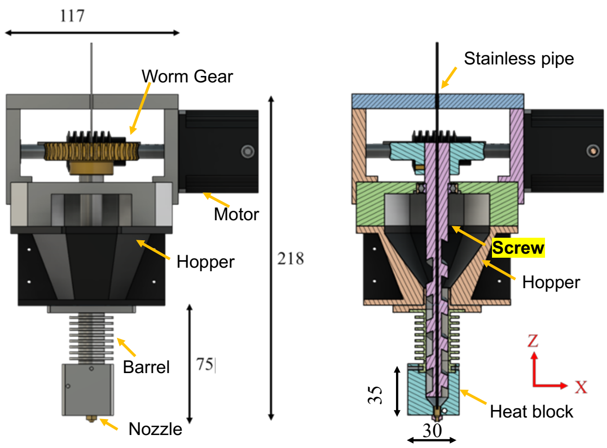

Fig. 2 Dimensions and cross-sectional view of the print head in reference [7].

2.2 Effects of heating

Ueda et al. [8] developed a new 3D printer that can fabricate continuous carbon fiber composites by using a heating compression roller. They fabricated tensile specimens using a continuous carbon fiber filament produced by Markforged. X-ray CT observations showed that the void was 10% when the heating compression roller was not used, but the void ratio was reduced to 3% by using the heating compression roller.

Imaeda et al. [9] simulated FFF 3D printing of a short carbon fiber/PA-6 composite material by using the modified MPS method, which is a particle simulation method. As the modified MPS method includes latent heat for the thermal conduction simulations, the flow of the thermoplastics can be simulated with high accuracy.

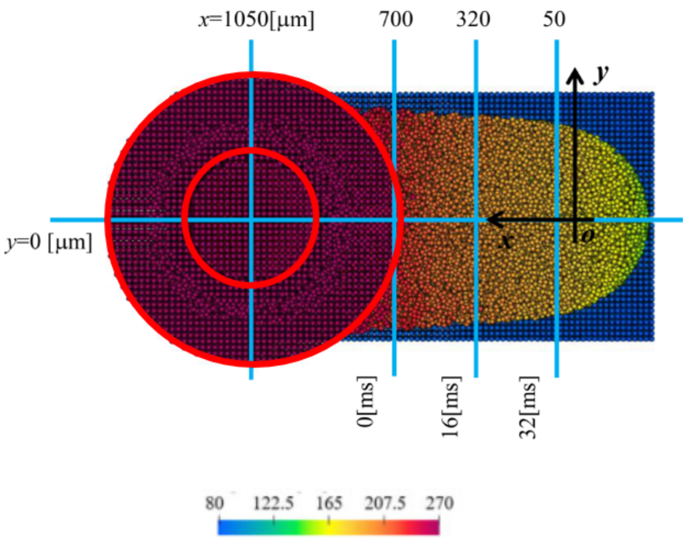

Fig. 3 Top view of the MPS computational results of temperature at the end of printing. The x–y coordinate origin is located at the center of the initial nozzle location, and each blue line indicates the nozzle location at the time. (Figure 4 from reference [9])

Figure 3 shows the changes in temperature when printing Onyx® (melting point, 221°C) and Markforged short carbon fiber/PA-6 composite filament [9]. The red circles on the left of the figure indicate the nozzle, which shows the area at approximately 270°C (this temperature exceeds the melting temperature of PA-6). This area is located 700 mm away from the origin O of the y-coordinate system (the origin indicates the nozzle center position at time 0). In the 320-mm line, 16 ms after the nozzle has passed, the color of the particle changes to orange, and the particles become solid below 200°C. This finding indicates that the liquid thermoplastic flow occurs only directly under the nozzle.

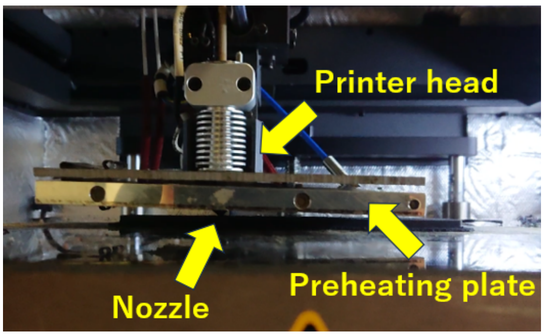

Fig. 4 Preheating plate mounted on the printer head. (Reference [10])

As shown in Fig. 4, Kubota et al. [10] experimentally investigated the effects of preheating by attaching a preheating plate to the print head. They used short carbon fiber/PEEK composites with a fiber volume fraction of 24% and measured the tensile strength of the lay-up direction with and without preheating. Consequently, preheating increased the tensile strength of the lay-up direction by 10 times.

As carbon fiber composites have a higher thermal conductivity than thermoplastics, performing heating and compression during printing is necessary to increase the fluidity of the melted thermoplastic, reduce voids, and increase the interlaminar strength. However, the weight of the screw-type print head is 1 kg. Thus, installing a heavy compression roller is not practical. In addition, the installation of a preheating plate leads to a significant increase in weight, which is also impractical. In this study, the nozzle cap was adopted instead. Although the nozzle cap cannot apply pressure to the printing pass, we cannot exclude the effect of pressurization, in which the resin extruded from the nozzle cannot move upward behind the nozzle movement direction.

2.3 Nozzle cap proposal and verification

Based on the results shown in Fig. 3 in which the nozzle rim is heating the printed pass, a nozzle cap was devised because the heat of the heat block could be transferred to a wider area around the nozzle rim. The nozzle cap is effective; thus, it can be applied to the existing 3D printers. Figure 5 shows a conceptual diagram of the nozzle cap. As shown in Fig. 2, the dimensions of the heat block part of the screw-type coaxial twin nozzles are larger than those of the normal 3D printer because the screw and heater are built-in. Therefore, a disc-shaped heat block extension jig with a diameter of approximately 9 mm and a thickness of 4.5 mm at the same height as the nozzle end was fabricated using the same aluminum alloy A5052 as the heat block. In the study conducted by Todoroki et al. [7], a nozzle with a diameter of 2.5 mm was used.

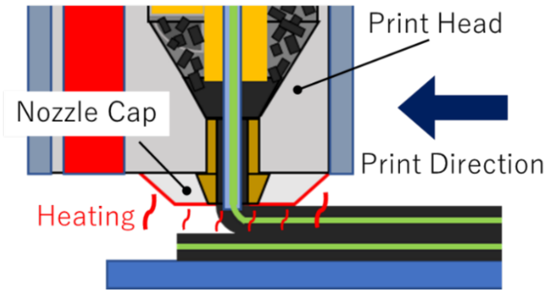

Fig. 5 Schematic representation of the nozzle cap.

The nozzle cap transmits the heat of the heat block to the print path and simultaneously preheats the underlying print path. The 3D image of the nozzle cap is shown in Fig. 6. The design drawing and processing method are shown in the appendix. The nozzle cap has a base of 20 × 20 mm square, and four holes with a diameter of 2 mm are drilled at the corners of the base. The nozzle cap is attached to the heat block with M2 bolts. A hole with a diameter of 2.6 mm is drilled at the center, and the nozzle head is designed so that the nozzle head comes out on the surface of the nozzle cap. Figure 7 shows a conceptual and cross-sectional view of the nozzle and nozzle cap attached to the heat block. Figure 8 shows the photos of the print head.

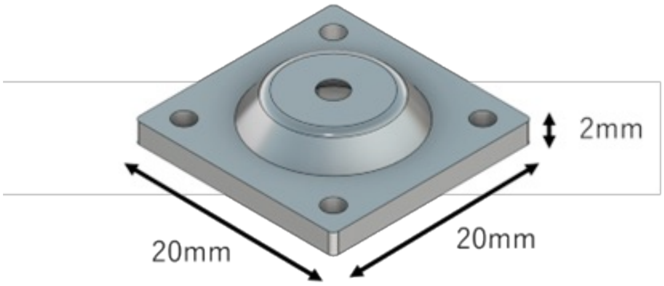

Fig. 6 3D model of the nozzle cap.

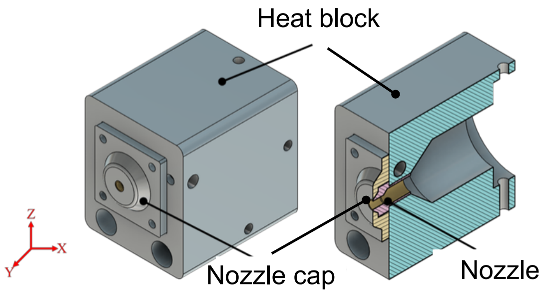

Fig. 7 Heat block and cutting model with the nozzle cap.

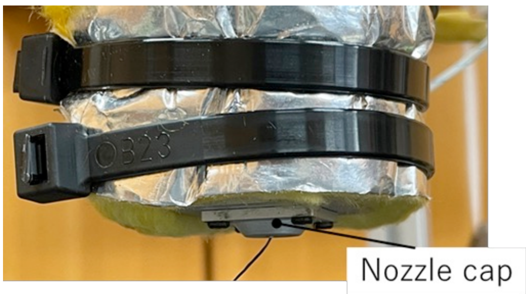

(a) 3D printer head with the nozzle cap.

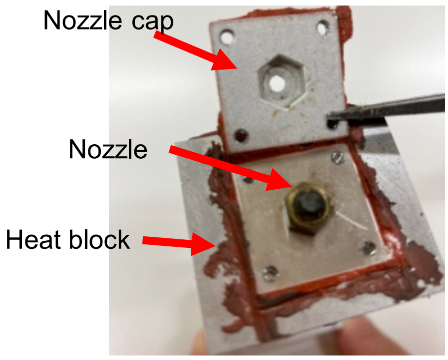

(b) Set up of the nozzle cap. Almost no gap is found between the nozzle and the nozzle cap.

Fig. 8 Photos of the nozzle cap.

In confirming the effectiveness of heating, the Markforged CFRP filament for MarkTwo® (fiber volume content of about 30%) was used as a continuous fiber filament, and 3DX Tech's Carbon Fiber Nylon 6 pellet was used as a short fiber–reinforced resin pellet. As shown in reference [7], the temperature of the nozzle cap was increased to 240°C, similar to the melting temperature. The temperature of the nozzle cap was measured (Fig. 9), where the temperature of the nozzle cap reached 238°C, demonstrating that the heating device is sufficient.

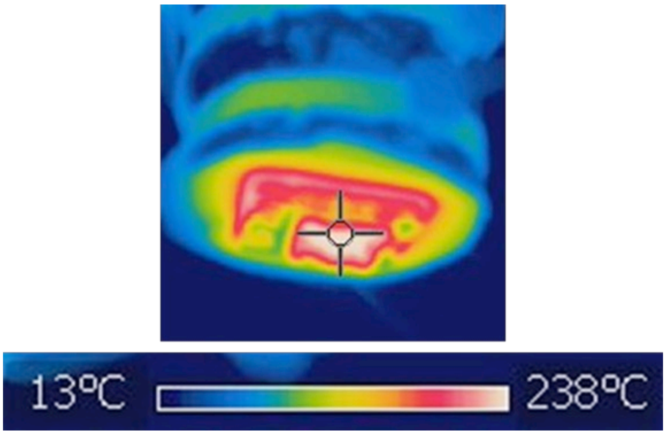

Fig. 9 Measured temperature results of the nozzle cap.

In evaluating the effectiveness of the nozzle cap, a single pass was printed with and without the nozzle cap. The cross-sectional observations of both cases were performed. The printing conditions are shown in Table 1. As shown in reference [7], the tip of the internal nozzle pipe was set to protrude 0.2 mm beyond the tip of the outer screw nozzle. This design will ensure that the continuous fiber path is wrapped in the short carbon fiber/PA-6.

Table 1. 3D printing conditions.

Nozzle temperature [°C]	240
Printing speed [mm/min]	100
Layer height [mm]	0.6
Print path distance [mm]	2.4

The results of the cross-sectional observation are shown in Fig. 10. The yellow arrows show the path of the continuous fiber. The void between the short-fiber-reinforced thermoplastic resin and the continuous fibers is greatly improved by using the nozzle cap. This result is due to the improved fluidity of the thermoplastic resin after printing, which reduced the voids between the short-fiber-reinforced resin and the continuous fibers. Based on the results, the effectiveness of the nozzle cap was confirmed in the cross-sectional observations of the single print pass.

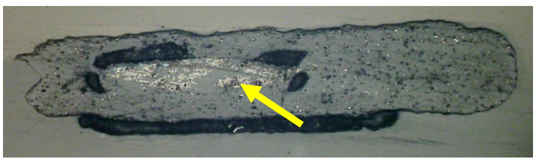

(a) Without the nozzle cap.

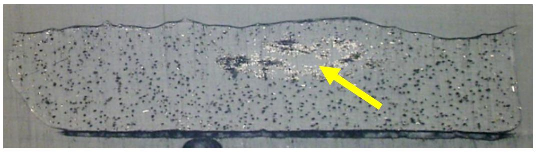

(b) With the nozzle cap.

Fig. 10 Cross-sectional image of the hybrid composite.

3. Verification of Effectiveness by Using a Strength Test

In demonstrating the effectiveness of the nozzle cap, fiber direction tensile tests (0° tensile tests) and interlaminar shear tests were performed with and without the nozzle cap. The results were compared, and the void ratios of the specimen cross-sections with and without the nozzle cap were measured to confirm the reduction of the void ratio.

3.1 0° Tensile Specimens

The fabrication method of the 0° tensile specimen in which the continuous fibers coincide with the tensile orientation is the same as that reported by Todoroki et al. [7] (Fig. 11).

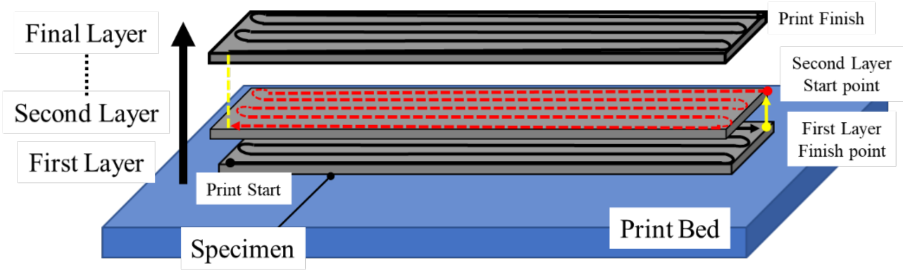

Fig. 11 Print path for the fabrication of unidirectional composite specimens. (Reference [7])

As shown in Fig. 11, the fibers were laminated without cutting. The specimen dimensions are 120 mm long × 16.8 mm wide × 2.4 mm thick; the distance between the print paths is 2.4 mm; the lamination pitch is 0.6 mm, and the lamination has four layers. After printing, both ends of the specimen were cut to eliminate the influence of the curved fibers at the end. Consequently, 0° tensile test specimens were fabricated. The tensile tests were performed by attaching 1.5-mm-thick GFRP tabs to the 25-mm part of both ends of the specimens. The tests were performed after keeping the specimen in a desiccator maintained at a humidity of 10% or less for at least 72 h to avoid the effects of moisture absorption.

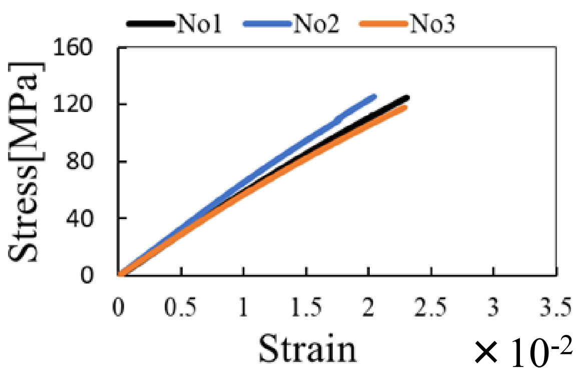

Fig. 12 Tensile test results of the 0° specimens fabricated with the nozzle cap.

The stress–strain diagram of the three specimens obtained in the tensile tests is shown in Fig. 12. The averaged tensile strength was 122.8 MPa, and the standard deviation was 3.53 MPa. The averaged elastic modulus was 6.13 GPa, and the standard deviation was 0.35 GPa. Todoroki et al. (7) reported the 0° tensile tests without the nozzle cap with a pass spacing of 2.4 mm. The averaged tensile test result was 121.4 MPa with SD of 6.14 MPa. For the 0° tensile tests, no difference is observed as the strength of the continuous carbon fibers is dominant.

3.2 Void ratio measurement

In measuring the void ratio, cross-sectional observations of the 0° tensile tests containing continuous fibers printed with and without the nozzle cap were performed. The specimens in this study comprised continuous carbon fiber composites and short carbon fiber composites; thus, the void ratios of both specimens were measured from the cross-sectional image without using the combustion method.

Todoroki et al. (7) reported that the void ratio of the specimen without using the nozzle cap was 6.8% (Fig. 13). Van Der Klift et al. (4) mentioned that the void ratio was about 7% from the cross-sectional observation of the MarkOne continuous fiber specimens of Markforged. The void ratio when the nozzle cap is not used was almost the same as that of Markforged.

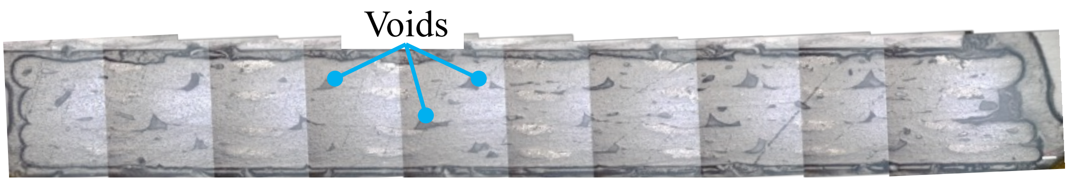

Fig. 13 Cross-sectional observation of the 0° specimen without the nozzle cap. (Reference [7]).

Fig. 14 Cross-sectional view of the specimen when the nozzle cap is used. Based on the result of the void ratio measurement by ImageJ, the void ratio was 2.16%, and the cross-sectional observation that the gap between the passes was reduced was compared with the case where the nozzle cap was not used.

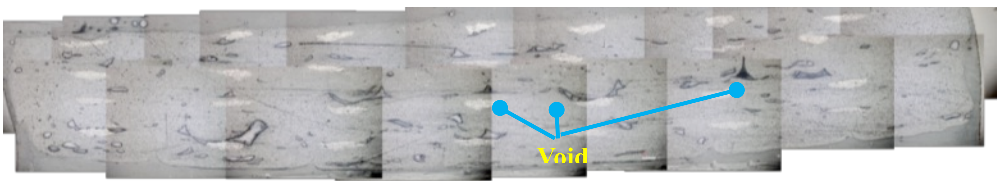

Fig. 14 Cross-sectional observation of the 0° specimen with the nozzle cap.

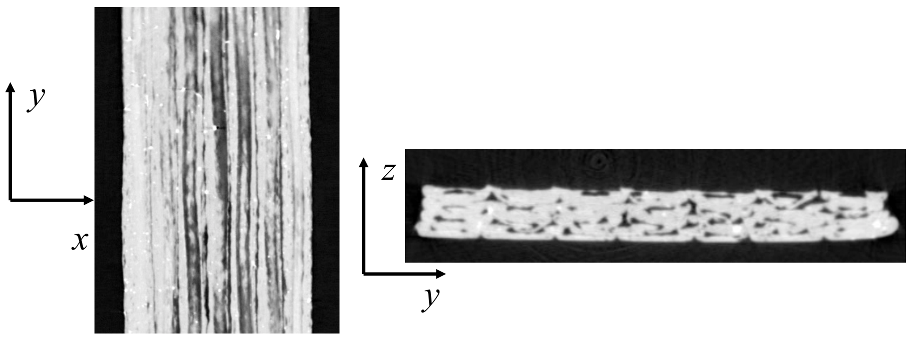

(a) Without the nozzle cap.

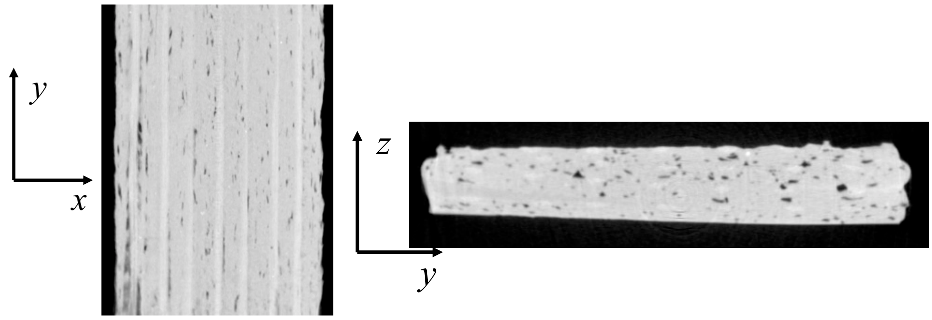

(b) With the nozzle cap.

Fig. 15 X-ray computed tomography (X-ray CT) results of the two types of specimen cross-sections.

The inside of the specimens used in the cross-sectional observations was examined using X-ray CT (Comscan Techno, ScanXmate-L080HT, pixel 50 μm). Figure 15 shows the X-ray CT observation results. As shown in Fig. 15 (a), the X-ray CT observation results indicate that a long gap occurs in the fiber direction between the passes because of the lack of resin flow when the specimen was printed without the nozzle cap. Figure 15 (b) shows that the print path heating with the nozzle cap promotes the flow of the melted thermoplastic resin between the passes and remarkably reduces the void.

3.3 Interlaminar shear test

Rectangular plates (30 mm long × 14.4 mm wide × 3 mm thick) were printed and used for interlaminar shear strength (ILSS) tests. The edges of the plates were cut to remove the effect of the curved continuous fiber. The specimen used for the ILSS test was 21 mm long × 12 mm wide × 3 mm thick. The printing path of the specimen was similar to that of the 0° tensile specimen (Fig. 11). The specimen configuration of the ILSS test is shown in Fig. 16. The setup of the ILSS test in the three-point bending form is shown in Fig. 17. The coordinates shown in Fig. 17 indicate the orientation at printing: The *x*-axis is the continuous carbon fiber direction; the *y*-axis is perpendicular to the fiber direction, and the z-axis is the lay-up direction. ILSS tests with a three-point bending type jig and a distance of 15 mm were conducted by using the universal testing machine AUTOGRAPH AG-I 100kN (SHIMADZU), and the test speed was 1 mm/min based on JIS K7078.

The results of the specimen printed without the nozzle cap are shown in Fig. 17, and the result of the specimen printed with the nozzle cap is shown in Fig. 18.

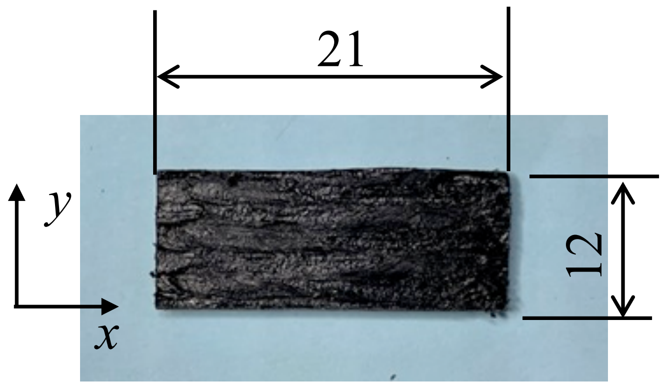

Fig. 16 Configuration of the ILSS specimens.

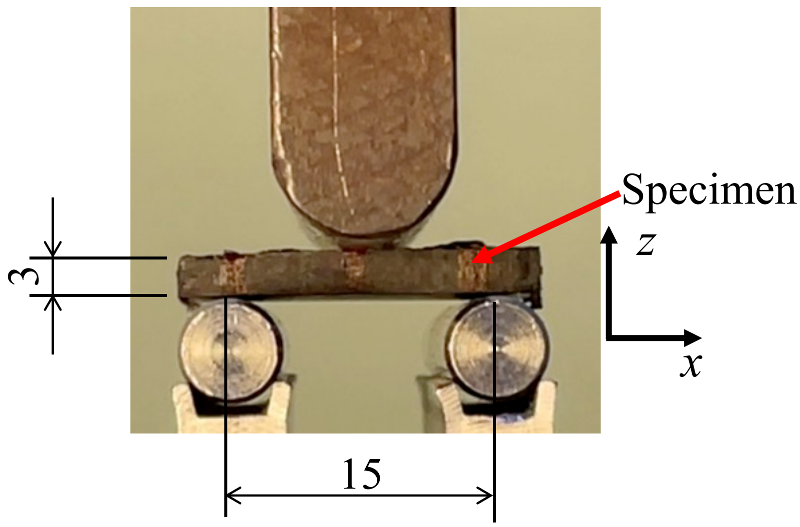

Fig. 17 ILSS test of the three-point-bending type.

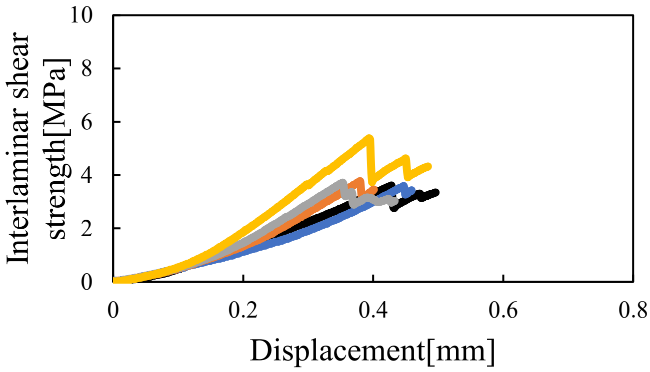

Fig. 18 Results of the ILSS test conducted on specimens printed without the nozzle cap.

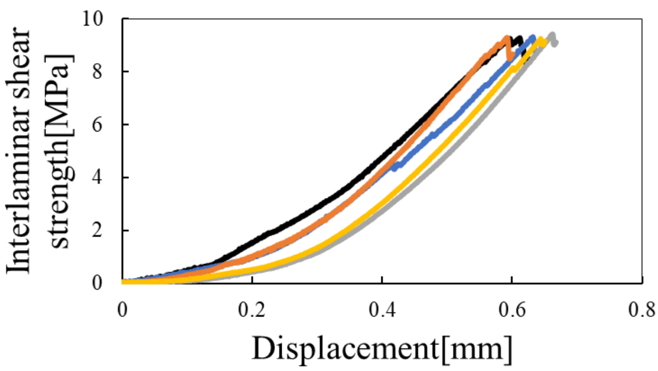

Fig. 19 Results of the ILSS test conducted on specimens printed with the nozzle cap.

As shown in Fig. 18, the mean value of the ILSS result was 3.98 MPa, and the SD was 0.61 MPa. As shown in Fig. 19, the mean value of the ILSS result was 9.31 MPa, and the SD was 0.05 MPa. The ILSS increased by 2.3 times by using the nozzle cap.

No damage was observed in the specimen printed without the nozzle cap after the ILSS test. Therefore, cross-sectional observation was performed using X-ray CT, and the result is shown in Fig. 20. As shown in Fig. 20, the coordinates show the direction of printing. The grip part during X-ray CT imaging was located at the left edge, and a delamination crack was located slightly to the left of the center of the figure.

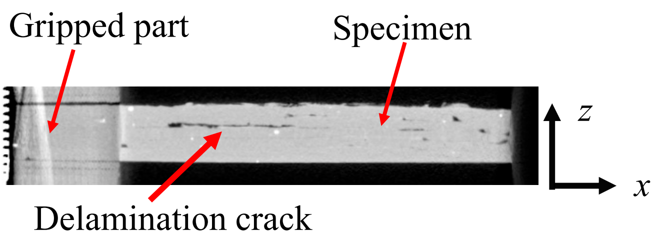

Fig. 20 X-ray CT observation of the ILSS specimens printed without the nozzle cap.

The specimen printed with the nozzle cap had a high ILSS. Thus, delamination occurred simultaneously from multiple defects, and it propagated to the specimen edge. In addition, the plastic deformation of the specimen was due to bending (Fig. 21). The orange triangles shown in Fig. 21 are the loading points. White is painted to the side of the specimen for observation.

As described above, during the ILSS test, the fracture was delaminated regardless of the usage of the nozzle cap.

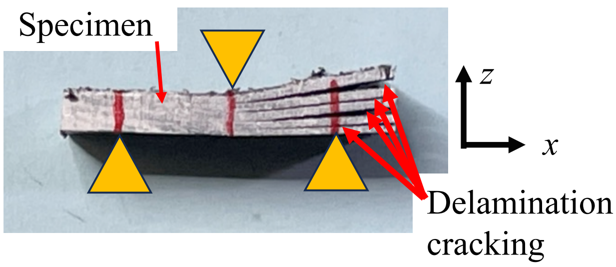

Fig. 21 Delamination cracking of the ILSS specimens printed with the nozzle cap.

3.4 Discussion

During the 0° tensile test, no difference in strength was observed because it depended on the fiber strength. However, the cross-sectional observation showed that the void was significantly reduced from 6.8% to 2.16%. The ILSS of the specimen printed with the nozzle cap increased by 2.3 times. The void ratio reduction is similar to the research result using the compaction roller in reference [(8)]. The increase of the nozzle tip diameter to 9.2 mm using the nozzle cap promotes the flow of the thermoplastic resin, and fusion occurs between the layers. However, this nozzle cap is currently designed on a trial-and-error basis. When the nozzle cap is too large, the thermoplastic resin sticks to the nozzle cap. Figure 22 shows the nozzle cap surface after printing. The resin has adhered to the cap. Therefore, designing a more optimal nozzle cap is a future challenge.

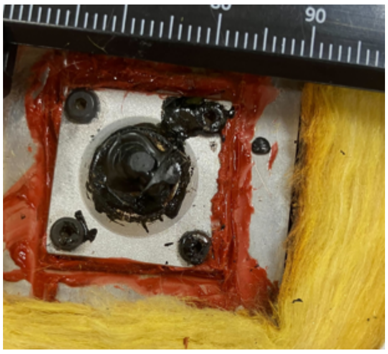

Fig. 22 Thermoplastic resin adhesion to the nozzle cap after 3D printing of the specimen.

4. Conclusion

In the previous study, a screw-type coaxial twin-nozzle 3D printer was developed. The insufficient flow of the thermoplastic resin caused a high void ratio and low interlamina strength. In addressing these problems, a nozzle cap method was developed, which serves as an extension of the heating section around the nozzle, heating the print pass and promoting the flow of the thermoplastic resin to reduce voids between the print passes. After heating the prototype nozzle and observing single-pass printing, 0° tensile tests were performed, and the void ratio was measured. Interlaminar shear tests were performed by comparing the specimens printed with the nozzle cap with those without the nozzle cap. The following results were obtained:

(1) The limitations of the current FFF method were addressed, and a nozzle cap that extends the tip of the nozzle by transmitting the heat of the heat block was proposed. The effectiveness of the nozzle cap was demonstrated by observing the cross-section of the single-pass print pass comprising a continuous carbon fiber filament and short carbon fiber/PA-6 pellets.

(2) 0° tensile tests and cross-sectional observation were conducted, and the nozzle cap showed no effect on the 0° tensile strength. However, the void ratio was reduced to the 2% range.

(3) Interlaminar shear tests were conducted, and the result showed that the ILSS increased by 2.3 times by using the nozzle cap.

Acknowledgements

We received the support of AGC Co., Ltd., in some parts of the experiments.

Appendices

The design drawing of the nozzle cap is shown in Fig. A-1. The height of the truncated cone of the nozzle cap matched the height of the nozzle. The cavity in the nozzle cap was adjusted to the nozzle shape in this study. However, if the heat transfer from the heat block is sufficient, then a cylindrical cavity can be made by sealing it with heat-resistant silicone rubber at the tip of the nozzle.

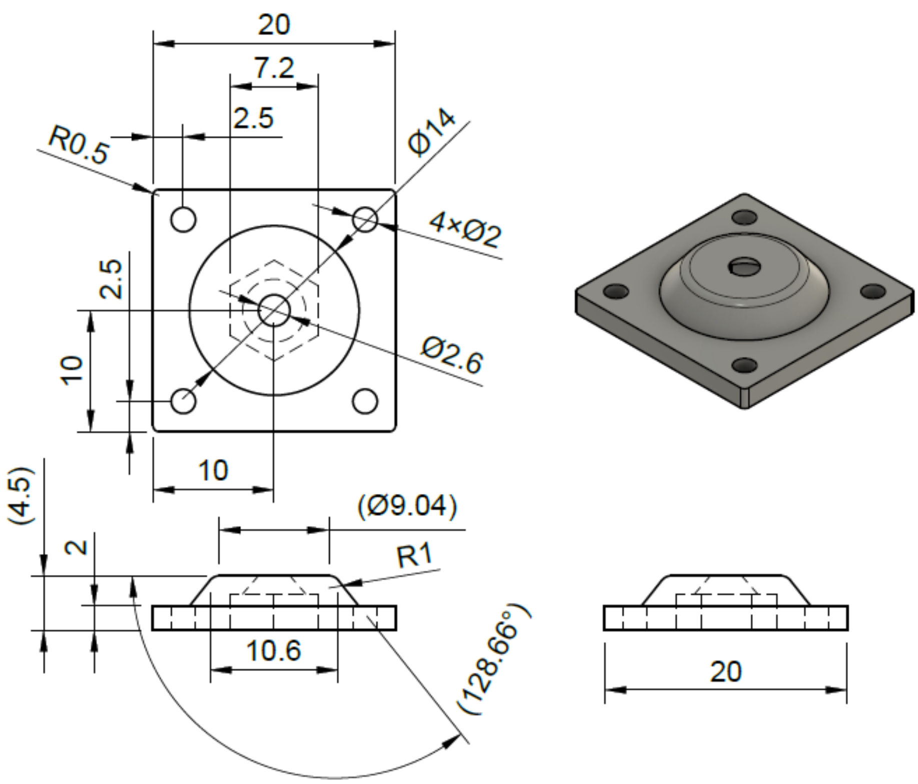

Fig. A-1 Engineering drawing of the nozzle cap.

References

(1) Schmitz B. https://www.3dcadworld.com/worlds-first-carbon-fiber-3d-printer-makes-debut-solidworks-world/, 2014 (Access 2024/5/14).

(2) Matsuzaki R, Ueda M, Namiki T, Jeong T, Asahara H, Horiguchi K, Nakamura T, Todoroki A, Hirano Y. Three-dimensional printing of continuous-fiber composites by in-nozzle impregnation. Scientific Reports. 2016;6:23058.

(3) Tian X, Liu T, Yang C, Wang Q, Li D. Interface and performance of 3D printed continuous carbon fiber reinforced PLA composites. Composites Part A: Applied Science and Manufacturing. 2016;88:198-205.

(4) Van Der Klift F, Koga Y, Todoroki A, Ueda M, Hirano Y, Matsuzaki R. 3D printing of continuous carbon fiber reinforced thermos-plastic (CFRTP) tensile test specimen. Open Journal of Composite Materials. 2016;6:18-27.

(5) Akira T, Itsuki O, Yoshihiro M, Yoshio S, Masato U, Ryosuke M, Yoshitaka H. 3D tensile test properties of continuous carbon fiber reinforced thermoplastic composites. Journal of the Japan Society for Composite Materials, Japan. 2019;45:141-148.

(6) Yamanaka Y, Todoroki A, Ueda M, Hirano Y, Matsuzaki R. Fiber line optimization in single ply for 3D printed composites. Open Journal of Composite Materials. 2016;6:121-131.

(7) Akira T, Kota H, Masato U, Ryosuke M, Keisuke I. A new 3D printer for continuous fiber composite molding using coaxial double nozzles. Agora of Additive Manufacturing. 2024;24001.

(8) Ueda M, Kishimoto S, Yamawaki M, Matsuzaki R, Todoroki A, Hirano Y, Le Duigou A. 3D compaction printing of a continuous carbon fiber reinforced thermoplastic. Composites Part A. 2020;137; 105985.

(9) Imaeda Y, Todoroki A, Matsuzaki R, Ueda M, Hirano Y. Modified moving particle semi-implicit method for 3D print process simulations of short carbon fiber/polyamide-6 composites. Composites Part C. 2021;6;100195.

(10) Masasuke K, Akira T, Kota H. Lamination orientation reinforcement by preheating 3D printed short carbon fiber PEEK. Reinforced Plastics. 2021;67;440-446.